Lattice Independent Component Analysis for fMRI analysis

Manuel Graña*, Maite García-Sebastián, Carmen Hernández

Grupo de Inteligencia computacional,
www.ehu.es/ccwintco
University of the Basque Country

Abstract. Pursuing an analogy to the Independent Component Analysis (ICA) we propose a Lattice Independent Component Analysis (LICA), where ICA signal sources correspond to the so-called endmembers and the mixing matrix corresponds to the abundance images. We introduce an approach to fMRI analysis based on a Lattice Computing based algorithm that induces endmembers from the data. The endmembers obtained this way are used to compute the linear unmixing of each voxel's time series independently. The resulting mixing coefficients roughly correspond to the General Linear Model (GLM) estimated regression parameters, while the set of endmembers corresponds to the GLM design matrix. The proposed approach is model free in the sense that the design matrix is not fixed *a priori* but induced from the data. Our approach does not impose any assumption on the probability distribution of the data. We show on a well known case study that this unsupervised approach discovered activation patterns are similar to the ones detected by an Independent Component Analysis (ICA).

1   Introduction

Human brain mapping is a rapidly expanding discipline, and in recent years the interest in novel methods for imaging human brain functionality has grown. Noninvasive techniques can measure cerebral physiologic responses during neural activation. One of the relevant techniques is functional Magnetic Resonance Imaging (fMRI) [13], which uses the blood oxygenation level dependent (BOLD) contrast to detect physiological alterations, such as neuronal activation resulting in changes of blood flow and blood oxygenation. Since these methods are completely noninvasive, using no contrast agent or ionizing radiation, repeated single-subject studies are becoming feasible [12].

The fMRI experiment consists of a functional template or protocol (e.g., alternating activation and rest for a certain time) that induces a functional response in the brain.The aim of an fMRI experiment is to detect the response to this time varying stimulus, through the examination of the signal resulting from the BOLD effect, in a defined volume element (voxel). The functional information of a voxel has to be extracted from its time series. One fMRI volume is recorded at each sampling time instant during the experiment. The frequency of the time sampling being determined by the

resolution of the fMRI imaging pulse sequence. The complete four-dimensional dataset (three spatial dimensions plus one time dimension) consists of subsequently recorded three-dimensional (3-D) volumes. The acquisition of the complete series of functional volumes runs over periods lasting up to several minutes.

The most extended analysis approach for fMRI signals is the Statistical Parametric Maps (SPM) [5,6] which has evolved into a free open source software package. This method consists in the separate voxel estimation of the regression parameters of General Linear Model (GLM), whose design matrix has been built corresponding to the experimental design. A contrast is then defined on the estimated regression parameters, which can take the form of a t-test or an F-test. The theory of Random Fields is then applied to correct the test thresholds, taking into account the spatial correlation of the independent test results.

Approaches to fMRI analysis based on the Independent Component Analysis (ICA) [4] assume that the time series observations are linear mixtures of independent sources which can not be observed. ICA assumes that the source signals are non-Gaussian and that the linear mixing process is unknown. The solutions to the ICA problem obtain both the independent sources and the linear unmixing matrix. These approaches are unsupervised because no *a priori* information about the sources or the mixing process is included, hence the alternative name of Blind Deconvolution.

In the present work we propose the use of an heuristic algorithm, called Endmember Induction Heuristic Algorithm (EIHA) described in detail in [7] to attack the fMRI analysis problem. The basic assumption in this approach is that the data is generated by a hidden process as a convex combination of a set of endmembers which are the vertices of a convex polytope covering the data observations. This assumption is similar to the linear mixture assumed by the ICA approach, however EIHA does not impose any probabilistic assumption on the data. This EIHA algorithm falls more properly in the field of Lattice Computing algorithms [8]. The endmembers discovered by the EIHA are equivalent to the GLM design matrix columns, and the unmixing process is identical to the conventional least squares estimator. Therefore, our approach is a kind of unsupervised GLM whose regressor functions are discovered in the data. When we establish an analogy with the ICA, the endmembers correspond to the unknown ICA sources and the mixing is solved by least squares estimation.

We call Lattice Independent Component Analysis (LICA) the overall process of applying EIHA and computing the unmixing process that gives the abundance matrices (in remote sensing terminology). The EIHA relies on the conjecture that Strong Lattice Independent sets of vectors are Affine Independent, and, therefore, the vertices of the convex polytope that explains (contains) the data. The algorithm searches for these Strong Lattice Independent vectors by using the properties of Lattice Autoassociative Memories (LAM). The main advantages that LICA can produce respect to ICA for data analysis are the lack of strong probabilistic assumptions (independence, non-Gaussianity) that may fail in many realistic situations. Besides the EIHA is a computationally light algorithm that works on one pass over the data and does not need optimization steps.

The outline of the paper is as follows: Section 2 introduces the linear mixing model so that the proposed approach can be understood. Section 3 presents an sketch of the

theoretical relation between Lattice Independence and Linear (Affine) Independence through the LAM theory. Section 4 recalls the definition of our Endmember Induction Heuristic Algorithm (EIHA). Section 5 gives a brief recall of ICA. Section 6 presents results of the proposed approach on a case study. Section 7 provides some conclusions.

2   The linear mixing model

The linear mixing model can be expressed as follows: $\mathbf{x} = \sum_{i=1}^{M} a_i \mathbf{s}_i + \mathbf{w} = \mathbf{Sa} + \mathbf{w}$, where $\mathbf{x}$ is the d-dimension pattern vector corresponding to the fMRI voxel time series vector, $\mathbf{S}$ is the $d \times M$ matrix whose columns are the d-dimension vertices of the convex region covering the data corresponding to the so called endmembers $\mathbf{s}_i, i = 1, .., M$, $\mathbf{a}$ is the M-dimension fractional abundance vector, and $\mathbf{w}$ is the d-dimension additive observation noise vector. The heuristic algorithm EIHA described in [7] provides the estimation of the endmembers from the data. We can not review EIHA here due to the lack of space. The linear mixing model is subjected to two constraints on the abundance coefficients. First, to be physically meaningful, all abundance coefficients must be non-negative $a_i \geq 0, i = 1, .., M$. Second, to account for the entire composition, they must be fully additive $\sum_{i=1}^{M} a_i = 1$. That means that we expect the vectors in $\mathbf{S}$ to be affinely independent and that the convex region defined by them includes *all* the data points.

Once the convex region vertices have been determined the unmixing process is the computation of the matrix inversion that gives the coordinates of the point relative to the convex region vertices. The simplest approach is the unconstrained least squared error (LSE) estimation given by: $\widehat{\mathbf{a}} = \left(\mathbf{S}^T\mathbf{S}\right)^{-1} \mathbf{S}^T\mathbf{x}$. The coefficients that result from this equation do not necessarily fulfill the non-negativity and full additivity conditions. Moreover, the EIHA [7] always produces convex regions that lie inside the data cloud, so that enforcing the non-negative and additivity to one conditions would be impossible for some data points. Negative values are considered as zero values and the additivity to one condition is not important as long as we are looking for the maximum abundances to assign meaning to the resulting spatial distribution of the coefficients. These coefficients are interpreted as the regressor coefficients corresponding to the decomposition of the fMRI voxel time series into the set of endmembers. That is, high positive values are interpreted as high positive correlation with the time pattern of the corresponding endmember. The interpretation of the endmember time series pattern is rather straightforward in some cases (i.e. the background noise), but it is difficult in general. Therefore, the unmixing process aims to to find regions of related behavior, as it done in ICA-based studies [4].

3   Lattice Independence and Lattice Autoassociative Memories

The work on Lattice Associative Memories (LAM) stems from the consideration of the algebraic lattice structure $(\mathbb{R}, \vee, \wedge, +)$ as the alternative to the algebraic framework given by the mathematical field $(\mathbb{R}, +, \cdot)$ for the definition of Neural Networks computation. The operators $\vee$ and $\wedge$ denote, respectively, the discrete $\max$ and $\min$ operators (resp. $\sup$ and $\inf$ in a continuous setting). Given a set of input/output pairs

of pattern $(X, Y) = \left\{ \left(\mathbf{x}^\xi, \mathbf{y}^\xi \right) ; \xi = 1, .., k \right\}$, a linear heteroassociative neural network based on the pattern's cross correlation is built up as $W = \sum_\xi \mathbf{y}^\xi \cdot \left(\mathbf{x}^\xi \right)'$. Mimicking this constructive procedure [14,15] propose the following constructions of Lattice Memories (LM): $W_{XY} = \bigwedge_{\xi=1}^{k} \left[\mathbf{y}^\xi \times \left(-\mathbf{x}^\xi \right)' \right]$ and $M_{XY} = \bigvee_{\xi=1}^{k} \left[\mathbf{y}^\xi \times \left(-\mathbf{x}^\xi \right)' \right]$, where $\times$ is any of the $\boxtimes$ or $\boxtimes$ operators. Here $\boxtimes$ and $\boxtimes$ denote the $\max$ and $\min$ matrix product [14,15]. respectively defined as follows: $C = A \boxtimes B = [c_{ij}] \Leftrightarrow c_{ij} = \bigvee_{k=1,...,n} \left\{ a_{ik} + b_{kj} \right\}$, and $C = A \boxtimes B = [c_{ij}] \Leftrightarrow c_{ij} = \bigwedge_{k=1,...,n} \left\{ a_{ik} + b_{kj} \right\}$.

Definition 1. *Given a set of vectors* $\left\{ \mathbf{x}^1, ..., \mathbf{x}^k \right\} \subset \mathbb{R}^n$ *a linear minimax combination of vectors from this set is any vector* $\mathbf{x} \in \mathbb{R}^n_{\pm\infty}$ *which is a linear minimax sum of these vectors:* $x = \mathcal{L} \left(\mathbf{x}^1, ..., \mathbf{x}^k \right) = \bigvee_{j \in J} \bigwedge_{\xi=1}^{k} \left(a_{\xi j} + \mathbf{x}^\xi \right)$, *where J is a finite set of indices and* $a_{\xi j} \in \mathbb{R}_{\pm\infty} \; \forall j \in J$ *and* $\forall \xi = 1, ..., k$.

Definition 2. *The* linear minimax span *of vectors* $\left\{ \mathbf{x}^1, ..., \mathbf{x}^k \right\} = X \subset \mathbb{R}^n$ *is the set of all linear minimax sums of subsets of X, denoted* $LMS \left(\mathbf{x}^1, ..., \mathbf{x}^k \right)$.

Definition 3. *Given a set of vectors* $X = \left\{ \mathbf{x}^1, ..., \mathbf{x}^k \right\} \subset \mathbb{R}^n$, *a vector* $\mathbf{x} \in \mathbb{R}^n_{\pm\infty}$ *is* lattice dependent *if and only if* $x \in LMS \left(\mathbf{x}^1, ..., \mathbf{x}^k \right)$. *The vector* $\mathbf{x}$ *is* lattice independent *if and only if it is not lattice dependent on X. The set X is said to be* lattice independent *if and only if* $\forall \lambda \in \{1, ..., k\}$, $\mathbf{x}^\lambda$ *is lattice independent of* $X \backslash \left\{ \mathbf{x}^\lambda \right\} = \left\{ \mathbf{x}^\xi \in X : \xi \neq \lambda \right\}$.

Definition 4. *A set of vectors* $X = \left\{ \mathbf{x}^1, ..., \mathbf{x}^k \right\} \subset \mathbb{R}^n$ *is said to be* max dominant *if and only if for every* $\lambda \in \{1, ..., k\}$ *there exists and index* $j_\lambda \in \{1, ..., n\}$ *such that*

$$x_{j_\lambda}^\lambda - x_i^\lambda = \bigvee_{\xi=1}^{k} \left(x_{j_\lambda}^\xi - x_i^\xi \right) \forall i \in \{1, ..., n\}.$$

Similarly, X is said to be min dominant *if and only if for every* $\lambda \in \{1, ..., k\}$ *there exists and index* $j_\lambda \in \{1, ..., n\}$ *such that*

$$x_{j_\lambda}^\lambda - x_i^\lambda = \bigwedge_{\xi=1}^{k} \left(x_{j_\lambda}^\xi - x_i^\xi \right) \forall i \in \{1, ..., n\}.$$

Definition 5. *A set of lattice independent vectors* $\left\{ \mathbf{x}^1, ..., \mathbf{x}^k \right\} \subset \mathbb{R}^n$ *is said to be* strongly lattice independent *(SLI) if and only if X is max dominant or min dominant or both.*

Conjecture 1. [17] *If* $X = \left\{ \mathbf{x}^1, ..., \mathbf{x}^k \right\} \subset \mathbb{R}^n$ *is strongly lattice independent then X is affinely independent.*

4 Endmember Induction Heuristic Algorithm (EIHA)

Let us denote $\left\{ \mathbf{f} \left(i \right) \in \mathbb{R}^d ; i = 1, .., n \right\}$ the time series in fMRI voxels, $\overrightarrow{\mu}$ and $\overrightarrow{\sigma}$ are, respectively, the mean vector and the vector of standard deviations computed componentwise over the voxels, α the noise correction factor and E the set of already discovered vertices. The gain parameter α controls the amount of flexibility in the discovering

1. Shift the data sample to zero mean
   $\{\mathbf{f}^c(i) = \mathbf{f}(i) - \overrightarrow{\mu}; i = 1, .., n\}$.
2. Initialize the set of vertices $E = \{\mathbf{e}_1\}$ with a randomly picked sample. Initialize the set of lattice independent binary signatures $X = \{\mathbf{x}_1\} = \{(e_k^1 > 0; k = 1, .., d)\}$
3. Construct the LAM's based on the lattice independent binary signatures: M_{XX} and W_{XX}.
4. For each pixel $\mathbf{f}^c(i)$
   (a) compute the noise corrections sign vectors $\mathbf{f}^+(i) = (\mathbf{f}^c(i) + \alpha\overrightarrow{\sigma} > \mathbf{0})$ and $\mathbf{f}^-(i) = (\mathbf{f}^c(i) - \alpha\overrightarrow{\sigma} > \mathbf{0})$
   (b) compute $y^+ = M_{XX} \boxtimes \mathbf{f}^+(i)$
   (c) compute $y^- = W_{XX} \boxtimes \mathbf{f}^-(i)$
   (d) if $y^+ \notin X$ or $y^- \notin X$ then $\mathbf{f}^c(i)$ is a new vertex to be added to E, execute once 3 with the new E and resume the exploration of the data sample.
   (e) if $y^+ \in X$ and $\mathbf{f}^c(i) > \mathbf{e}_{y+}$ the pixel spectral signature is more extreme than the stored vertex, then substitute $\mathbf{e}_{y+}$ with $\mathbf{f}^c(i)$.
   (f) if $y^- \in X$ and $\mathbf{f}^c(i) < \mathbf{e}_{y-}$ the new data point is more extreme than the stored vertex, then substitute $\mathbf{e}_{y-}$ with $\mathbf{f}^c(i)$.
5. The final set of endmembers is the set of original data vectors $\mathbf{f}(i)$ corresponding to the sign vectors selected as members of E.

Algorithm 1: Endmember Induction Heuristic Algorithm (EIHA)

of new endmembers. The detailed description of the steps in the heuristic algorithm is presented as Algorithm 1. The starting endmember set consists of a randomly picked pixel. However, this selection is not definitive, because the algorithm may later change this endmember for another, more extreme, one. The noise correction parameter α has a great impact on the number of endmembers found. Low values imply large number of endmembers. It determines if a vector is interpreted as a random perturbation of an already selected endmember. This algorithm does not need a priori information about the nature of the data points that we want to detect. It runs once over the image and finds the most salient data samples on the fly. For this reason we say that it is an on-line algorithm.

5 Independent Component Analysis (ICA)

The Independent Component Analysis (ICA) [11] assumes that the data is a linear combination of non Gaussian, mutually independent latent variables with an unknown mixing matrix. The ICA reveals the hidden independent sources and the mixing matrix. That is, given a set of observations represented by a d dimensional vector $\mathbf{x}$, ICA assumes a generative model $\mathbf{x} = \mathbf{As}$, where $\mathbf{s}$ is the M dimensional vector of independent sources and $\mathbf{A}$ is the $d \times M$ unknown basis matrix. The ICA searches for the linear transformation of the data $\mathbf{W}$, such that the projected variables $\mathbf{Wx} = \mathbf{s}$ are as independent as possible. It has been shown that the model is completely identifiable if the sources are statistically independent and at least $M - 1$ of them are non Gaussian. If the sources are gaussian the ICA transformation could be estimated up to an orthogonal transformation. Estimation of mixing and unmixing matrices can be done maximizing diverse

objective functions, among them the non gaussianity of the sources and the likelihood of the sample. We have used the FastICA [10] algorithm available at http://www.cis.hut. /projects/ica/fastica.

Application of ICA to fMRI has been reviewed by [4]. Reports on the research application of ICA to fMRI signals include the identification of signal types (task related and physiology related) and the analysis of multisubject fMRI data. The most common approach is the spatial ICA that looks for spatial disjoint regions corresponding to the identified signal types. It has been claimed that ICA has identified several physiological noise sources as well as other noise sources (motion, thermodynamics) identifying task related signals. Diverse ICA algorithms have been tested in the literature with inconclusive results. Among them, fastICA, the one that we will apply in the case study, did identify the task related signals consistently. Among the clinical applications, ICA has been used to study the brain activation due to pain in healthy individuals versus those with chronic pain [1], the discrimination of Alzheimer's patients from healthy controls [9], the classification of schizophrenia [2] and studies about the patterns of brain activation under alcohol intoxication [3].

6 A case study

The experimental data corresponds to auditory stimulation test data of single person [1]. These data are the result of the preprocessing pipeline that removes many noise sources. These whole brain BOLD/EPI images were acquired on a modified 2T Siemens MAGNETOM Vision system. Each acquisition consisted of 64 contiguous slices. Each slice being a 2D image of one head volume cut. There are 64x64x64 voxels of size 3mm x 3mm x 3mm. The data acquisition took 6.05s, with the scan-to-scan repeat time (RT) set arbitrarily to 7s., 96 acquisitions were made (RT=7s) in blocks of 6, i.e., 16 blocks of 42s duration. The condition for successive blocks alternated between rest and auditory stimulation, starting with rest. Auditory stimulation was bi-syllabic words presented binaurally at a rate of 60 per minute. Due to T1 effects it is advisable to discard the first few scans (there were no "dummy" lead-in scans). We have discarded the first 10 scans.

Voxel time series are normalized susbtracting the mean value of each voxel time series independently, so that the plots are collapsed around the origin. This mean substraction corresponds to an scale normalization in the Lattice Computing sense. It removes scale effects that hinder the detection of meaningful lattice independent vectors. In the context of the GLM this normalization corresponds to the estimation of the voxel linear model offset.

The application of the EIHA algorithm with $\alpha = 20$ to the lattice normalized time series of the whole 3D volume produces the collection of eleven endmembers shown in figure 1. Attending to the intensity scale it can be assumed that the first endmember (top left plot) corresponds to the background (thermodynamical) noise, while the remaining endmembers correspond to some kind of hemodynamic response pattern or noise source. To identify the endmember which is closer to modeling the task, we compute the correlation of the endmembers with the square wave represent the task. We

---

[1] The dataset is freely available from ftp://ftp.fil.ion.ucI.ac.uk/spm/data, the file name is snrfM00223.zip. The functional data starts at acquisition 4, image snrfMOO223-004.

find that endmember #9 (counting row-wise in figure 1) has the maximum such correlation. We present in figure 2 the activations corresponding to it, where the slices shown roughly try to show the region of the auditory cortex were the task-related activations are expected. Top row is the axial and coronal cut, and the bottom row shows two sagital cuts at both sides of the brain. White voxels in this figure correspond to voxels with abundance value above the 99% percentile of the distribution of this endmember abundance over the whole volume. It can be appreciated that most of the activations fall in the auditory cortex region.
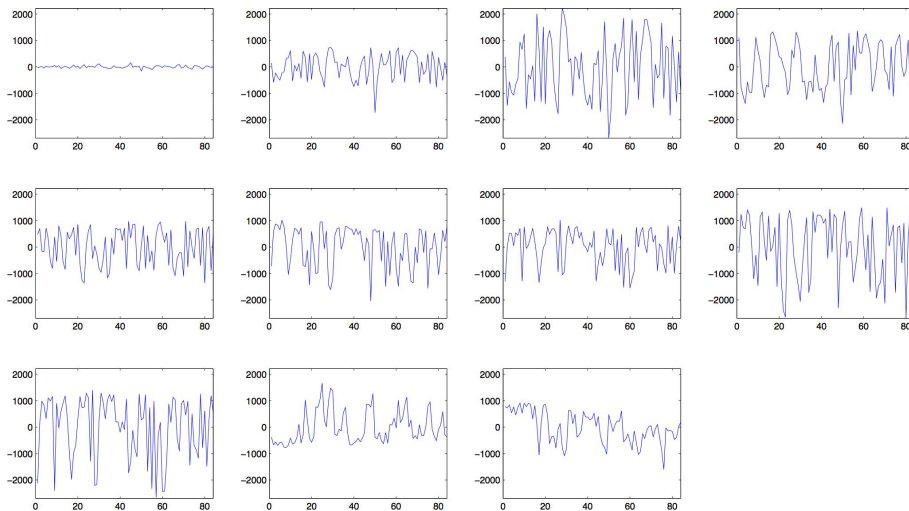

Fig. 1. Eleven endmbers detected by EIHA over the lattice normalized time series of the whole 3D volume.

The application of the fastICA algorithm with the number of sources set to 11, to match the number of endmembers found by the EIHA, to the lattice normalized time series of the whole 3D volume produces the collection of eleven endmembers shown in figure 3. Counting row-wise, source #8 may correspond to the background noise, while source #6 is the one most correlated with the task. Figure 4 shows the axial, coronal and sagital cuts corresponding to the auditory cortex, organized like in figure 2, with activation clusters, computed as the 99% percentile of the distribution of the spatial mixing values for source #6 over all the volume, superimposed. The task-related activations are localized in the auditory cortex, but they are less coherent than the EIHA found ones.

7   Conclusions and discussion

We have proposed and applied the endmember induction algorithm EIHA discussed in [7] to the model-free (unsupervised) analysis of fMRI. We have discussed the similarities of our approach to the ICA application to fMRI activation detection [4,18]. In our
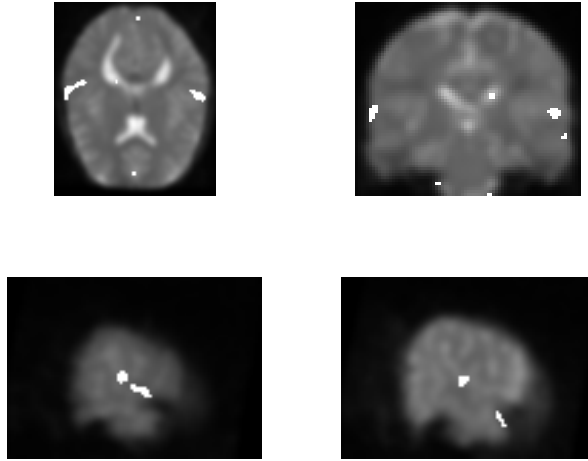
Fig. 2. Detected task related activations for endmember #9 from figure 1. White voxels correspond to abundance values above the 99% percentile of the distribution of the abundances for this endmember on the whole volume.
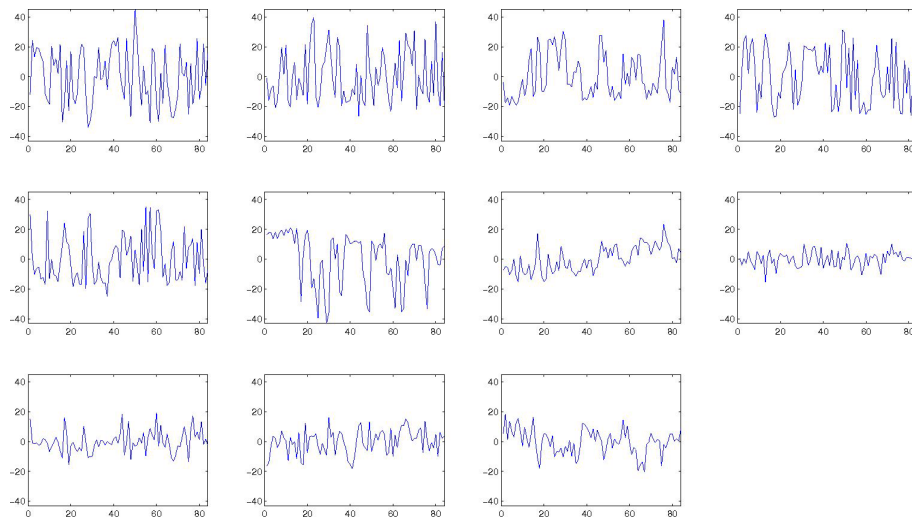

Fig. 3. Eleven time series sources detected by fastICA over the lattice normalized time series of the whole 3D volume.
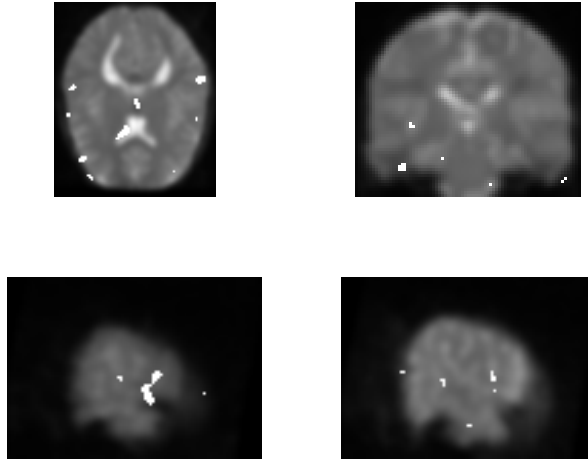
Fig. 4. Detected task related activations for source #6 from figure 3. White voxels correspond to mixing values above the 99% percentile of the distribution of the mixing coefficients for this source on the whole volume.

approach the temporal sources correspond to endmembers detected by the EIHA algorithm and the spatial mixing coefficients correpond to the abundance volumes obtained by unmixing the voxel time series on the basis of the found endmembers.

The first obstacle that we find in this endeavor is that the distribution of the fMIR voxel time series is not well aspected for the detection of Lattice Independence as a meaningful characteristic. In fact the voxel's fMRI time series show a dense distribution of intensity displacements from the origin, so almost all of them are lattice dependent and our proposed algorithm only identifies two endmembers on the raw data. To overcome this problem we apply a Lattice Normalization which corresponds to a scale normalization in the sense of Lattice Computing. We substract the mean of its time series to each voxel time series. The resulting lattice normalized data set shows a much more rich structure in terms of Lattice Independence. Our computational experiment with a well known fMRI data set, provided with the distribution of the SPM software, show some promising results in the sense that we can at least identify a task related endmember, and that other effects, such as thermodynamical noise, are also clearly identified. We have found also a strong agreement of the spatial localizations of a task related source found by the fastICA on the same dataset, with the ones provided by our approach. Future works must address works on clinical research, and the extension of the approach to groups and multiple groups.

References

1. A.L. Buffington, C.A. Hanlon, and M.J. McKeown, Acute and persistent pain modulation of attention-related anterior cingulate fMRI Activations, *Pain*,vol. 113, no. 12, pp. 172184, 2005.
2. V.D. Calhoun, K.A. Kiehl, P.F. Liddle, and G.D. Pearlson, Aberrant local- ization of synchronous hemodynamic activity in auditory cortex reliably character- izes schizophrenia, Biol. Psych., vol. 55, no. 8, pp. 842849, 2004. San Diego, CA, 2001, pp. 120125.
3. V.D. Calhoun, J.J. Pekar, and G.D. Pearlson, Alcohol intoxication effects on simulated driving: Exploring alcohol-dose effects on brain activation using func- tional MRI, Neuropsychopharmacology, vol. 29, no. 11, pp. 20972107, 2004.
4. V.D. Calhoun, T. Adali, T., Unmixing fMRI with independent component analysis, *Engineering in Medicine and Biology Magazine, IEEE* (2006) 25(2):79-90
5. K.J. Friston, A.P. Holmes, K.J. Worsley, J.P. Poline, C.D. Frith, R.S.J. Frackowiak, Statistical parametric maps in functional imaging: A general linear approach, *Hum. Brain Map.* (1995) 2(4):189-210
6. k.j. Friston, J.T. Ashburner, S.J. Kiebel, T.E. Nichols, W.D. Penny (eds.) *Statistical Parametric Mapping, the analysis of functional brain images*, Academic Press, 2007
7. M. Graña, I. Villaverde, J.O. Maldonado, C. Hernandez, Two Lattice Computing approaches for the unsupervised segmentation of Hyperspectral Images, *Neurocomputing* (2008) online publication DOI 10.1016/j.neucom.2008.06.026
8. M. Graña, A Brief Review of Lattice Computing, *Proc. WCCI 2008*, pp. 1777-1781
9. M.D.Greicius, G.Srivastava, A.L.Reiss, and V.Menon, Default-mode network activity distinguishes alzheimers disease from healthy aging: Evidence from func- tional MRI, Proc. Nat. Acad. Sci. U.S.A., vol. 101, no. 13, pp. 46374642, 2004.
10. Hyvarynën A., E. Oja, A fast fixed-point algorithm for independent component analysis, *Neural Comp.* 9:1483-1492, 1999
11. Hyvarynën A., J. Karhunen, E. Oja, *Independent Component Analysis*, John Wiley & Sons, New York, 2001
12. H.-P. Muller, E. Kraft, A. Ludolph, S.N. Erne, New methods in fMRI analysis, *Engineering in Medicine and Biology Magazine, IEEE*, (2002) 21(5):134-142
13. J.J. Pekar, A brief introduction to functional MRI, *Engineering in Medicine and Biology Magazine, IEEE* (2006) 25(2):24-26
14. G. X. Ritter , P. Sussner, J. L. Diaz-de-Leon. Morphological associative memories. *IEEE Trans. on Neural Networks*, (1998) 9(2):281–292,
15. G. X. Ritter , J. L. Diaz-de-Leon, P. Sussner. Morphological bidirectional associative memories. *Neural Networks*, (1999) 12, pp: 851–867,
16. G.X. Ritter, P. Gader, Fixed points of lattice transforms and lattice associative memories In: Hawkes P (ed.) *Advances in Imaging and Electron Physics* (2006) 144 pp. 165–242, Elsevier, San Diego, CA
17. G.X. Ritter, G. Urcid, M.S. Schmalz, Autonomous single-pass endmember approximation using lattice auto-associative memories *Neurocomputing* (2008) in press
18. G.E. Sarty, *Computing Brain Activation Maps from fMRI Time-Series Images*, Cambridge University Press, 2007